MYELOID NEOPLASIA

RUNX1/AML1 mutant collaborates with BMI1 overexpression in the development of human and murine myelodysplastic syndromes

Yuka Harada,[1] Daichi Inoue,[2] Ye Ding,[3] Jun Imagawa,[3] Noriko Doki,[2] Hirotaka Matsui,[4] Takashi Yahata,[5] Hiromichi Matsushita,[5] Kiyoshi Ando,[5] Goro Sashida,[6] Atsushi Iwama,[6] Toshio Kitamura,[2] and Hironori Harada[3]

[1]Division of Radiation Information Registry, Research Institute for Radiation Biology and Medicine, Hiroshima University, Hiroshima, Japan; [2]Division of Cellular Therapy, Advanced Clinical Research Center, Institute of Medical Science, University of Tokyo, Tokyo, Japan; [3]Department of Hematology and Oncology and [4]Department of Molecular Oncology, Research Institute for Radiation Biology and Medicine, Hiroshima University, Hiroshima, Japan; [5]Division of Hematopoiesis, Research Center for Regenerative Medicine, Tokai University School of Medicine, Isehara, Japan; and [6]Department of Cellular and Molecular Medicine, Graduate School of Medicine, Chiba University, Chiba, Japan

Key Points

- BMI1 overexpression is one of the second hit partner genes of RUNX1 mutations that contribute to the development of MDSs.

RUNX1/AML1 **mutations have been identified in myelodysplastic syndromes (MDSs). In a mouse bone marrow transplantation model, a RUNX1 mutant, D171N, was shown to collaborate with Evi1 in the development of MDSs; however, this is rare in humans. Using enforced expression in human CD34$^+$ cells, we showed that the D171N mutant, the most frequent target of mutation in the *RUNX1* gene, had an increased self-renewal capacity, blocked differentiation, dysplasia in all 3 lineages, and tendency for immaturity, but no proliferation ability. *BMI1* overexpression was observed in CD34$^+$ cells from the majority of MDS patients with RUNX1 mutations, but not in D171N-transduced human CD34$^+$ cells. Cotransduction of D171N and BMI1 demonstrated that BMI1 overexpression conferred proliferation ability to D171N-transduced cells in both human CD34$^+$ cells and a mouse bone marrow transplantation model. Stepwise transduction of D171N followed by BMI1 in human CD34$^+$ cells resulted in long-term proliferation with a retained CD34$^+$ cell fraction, which is quite similar to the phenotype in patients with higher-risk MDSs. Our results indicate that *BMI1* overexpression is one of the second hit partner genes of *RUNX1* mutations that contribute to the development of MDSs. (*Blood*. 2013;121(17):3434-3446)**

Introduction

The *RUNX1/AML1* gene has been investigated in the pathogenesis of hematopoietic diseases, and point mutations of *RUNX1* have been frequently detected in patients with various types of myeloid neoplasms. A heterozygous germ line mutation of the *RUNX1* gene is known to cause familial platelet disorder with a predisposition to acute myeloid leukemia (FPD/AML),[1,2] which is regarded as familial myelodysplastic syndromes (MDSs).[3] *RUNX1* mutations have been detected with high frequency in MDSs, MDSs following AML,[4] minimally differentiated AML M0 subtypes,[2,5-7] de novo AML without recurrent or complex karyotype,[8,9] and myelodysplastic/myeloproliferative neoplasms.[10,11] Furthermore, *RUNX1* mutations are detected with high frequency in therapy-related or radiation-associated MDSs and AML,[4,12-15] and leukemic transformation from myeloproliferative neoplasms.[16-19]

It is intriguing how RUNX1 mutations contribute to the development of divergent hematologic neoplasms. Functionally, most of the RUNX1 mutants equally show a loss of normal RUNX1 *trans*-activation potential.[4,12,20,21] The amino acid residues in the runt homology domain (RHD) of the RUNX1 protein that directly interact with DNA have been found to be frequent targets of amino acid replacement.[20,21] Mutations on other amino acids close to these DNA-contact residues are also suspected to inhibit DNA binding by an obstructive side-chain or a structural change. Therefore, amino-replacement and in-frame insertion/deletion types of mutations confer loss of DNA-binding ability and *trans*-activation potential. *RUNX1* mutations have been shown to play a pivotal role in the pathogenesis of MDS/AML in mouse bone marrow transplantation (BMT) systems.[22] Mice transduced with the D171N mutant, which harbors a mutation in the RHD of the *RUNX1* gene, exhibited hyperproliferative AML with multilineage dysplasia in collaboration with *Evi1* overexpression. This impressive result indicates that *RUNX1* mutations may be a cause of MDSs with a leukemogenic potential. However, mouse phenotypes do not always correspond to the clinical features of patients with the mutations. This may be partly due to differential gene circumstances, such as retrovirus integration sites or collaborating gene alterations, between mouse and human.[23,24] As opposed to *EVI1*, overexpression of the polycomb group gene *BMI1* is more common in MDS patients and is associated with MDS progression.[25,26] Biological analysis using human hematopoietic cells is considered to be necessary to clarify the molecular mechanisms of the *RUNX1* mutations in the pathogenesis of MDSs. Enforced gene expression in human CD34$^+$ cells has been used to investigate the role of leukemogenic oncogenes in leukemogenesis.[27-35]

Submitted June 3, 2012; accepted February 16, 2013. Prepublished online as *Blood* First Edition paper, March 7, 2013; DOI 10.1182/blood-2012-06-434423.

Y.H., D.I., and Y.D. contributed equally to this study.

The online version of this article contains a data supplement.

The publication costs of this article were defrayed in part by page charge payment. Therefore, and solely to indicate this fact, this article is hereby marked "advertisement" in accordance with 18 USC section 1734.

In this study, using enforced gene expression in human $CD34^+$ cells, we demonstrated that the D171N mutant, the most frequent target of mutation in *RUNX1* gene, has an increased self-renewal capacity, blocked differentiation, dysplasia in all 3 lineages, and tendency for immaturity, but no proliferation ability. Moreover, we revealed that *BMI1* overexpression collaborates with *RUNX1* mutations and confers proliferation ability to D171N-mutated cells, which was confirmed in both human and mouse hematopoietic stem/progenitor cells. Our results indicate that *BMI1* overexpression is one of the second hit partner genes of *RUNX1* mutations in the development of MDSs.

Materials and methods

Patients

Patients with MDSs were divided into 2 groups using the International Prognostic Scoring System: lower-risk MDSs include low- or intermediate-1-risk MDSs, and higher-risk MDSs include intermediate-2- or high-risk MDSs. Mutation analysis of *RUNX1* was performed as described previously.[4] The study was approved by the institutional review board at Hiroshima University. Patients gave written informed consent for the study, according to the Declaration of Helsinki.

Quantitative reverse-transcription polymerase chain reaction (qRT-PCR)

$CD34^+$ cells were purified from patients using the CD34 MicroBead Kit and autoMACS system (Milteny Biotec, Bergisch Gladbach, Germany). Total RNA was harvested from the $CD34^+$ cells using the RNeasy Micro Kit (Qiagen, Hilden, Germany). The expression levels of *EVI1*, *BMI1*, *INK4A*, *ARF*, and *GAPDH* were quantified by the Applied Biosystems 7500 Real-Time PCR system using TaqMan Gene Expression Assays (Hs00602795_m1 for *EVI1*, Hs00180411_m1 for *BMI1*, Hs00923894_m1 for *INK4A*, Hs99999189_m1 for *ARF*, and Hs99999905_m1 for *GAPDH*) and TaqMan Universal PCR Master Mix (Applied Biosystems). qRT-PCR in mouse cells was performed as described previously[22] with the following forward/reverse primer pairs: p16 (aatctccgcgaggaaagc/gtctgcagcggactccat), p19 (gggttttcttg gtgaagttcg/ttgcccatcatcatcacct), Evi1 (atcggaagatcttagatgagttttg/cttcctacatctggt tgactgg), and Gapdh (gcattgtggaagggctcatg/ttgctgttgaagtcgcaggag).

Retroviral vectors and infection

RUNX1 (wild-type [WT] and D171N mutant) cDNA with FLAG tag was subcloned into the pMXs-internal ribosomal entry site (IRES)-enhanced green fluorescent protein (EGFP) (pMXs.IG). *BMI1* was subcloned into the pMXs-IRES-DsRed-Express (pMXs.IR), in which the IRES-DsRed-Express fragment from the pIRES2-DsRed-Express (Clontech, Mountain View, CA) was inserted into the pMXs. FLAG-tagged D171N was also subcloned into pMYs-IRES-puro (pMYs.IP) and pMYs-IRES-EGFP (pMYs.IG), and *BMI1* into pMYs-IRES-blasticidin (pMYs.IB) and pMYs-IRES-nerve growth factor receptor (NGFR) (pMYs.IN). Plat-GP and Plat-E packaging cells were transfected with retroviral constructs using FuGENE6 (Roche, Mannheim, Germany) as described previously.[16,22]

Retrovirus transduction of human $CD34^+$ primary cells

Cord blood cells (CBs) were collected with written informed consent. $CD34^+$ cells were purified from CBs by the CD34 MicroBead Kit using autoMACS. They were precultured for 3 to 4 days in Stemline II Hematopoietic Stem Cell Expansion medium (Sigma-Aldrich, St Louis, MO) supplemented with 100 ng/mL each of Fms-related tyrosine kinase (FLT-3) ligand, stem cell factor (SCF), and thrombopoietin (TPO) (PeproTech, London, UK) (expansion medium). The cells were resuspended in new expansion medium and placed in plates coated with RetroNectin (Takara, Otsu, Japan) preloaded with virus. At 3 to 4 days after transduction, green fluorescent protein (GFP^+) and/or $DsRed^+$ cells were sorted by FACS Aria (Becton Dickinson [BD], Franklin Lakes, NJ).

Cells were cultured continuously in Iscove modified Dulbecco medium containing 20% fetal bovine serum and 100 ng/mL each of FLT-3 ligand, SCF, and TPO. For long-term growth, Iscove modified Dulbecco medium was supplemented with 20% fetal bovine serum; 100 ng/mL each of FLT-3 ligand, SCF, and TPO; and 20 ng/mL each of interleukin (IL) 6 and IL-3 (Peprotech).

Colony-forming cell (CFC) replating assay

Ten thousand sorted cells were resuspended in MethoCult $H4034^+$ medium (StemCell Technologies, Vancouver, BC, Canada) containing SCF, granulocyte colony-stimulating factor (G-CSF), granulocyte macrophage (GM)–CSF, IL-3, and erythropoietin. After 14 days in culture, colonies were counted. Cells were then suspended in methylcellulose medium, and 10^4 cells were plated again for CFC replating assay. The remaining cells were used for cell number counting and cytospin centrifuge for morphologic and flow cytometry analyses.

Long-term culture-initiating cell (LTC-IC) assay

For bulk culture assay, 10 000 sorted cells were suspended in Myelocult H5100 medium (StemCell Technologies) with 1 μM hydrocortisone (StemCell Technologies). The cells were divided into 2 dishes precoated with MS5 stromal cells and cultured for 5 weeks. LTC-IC cultures were harvested, and clonogenic progenitors were assayed in Methocult GF^+ H4435 medium (StemCell Technologies) containing SCF, GM-CSF, IL-3, IL-6, G-CSF, and erythropoietin. After 20 days, LTC-IC–derived CFCs were counted. For limiting dilution assay, 100 to 800 sorted cells per well were plated on MS5 stromal cells in 96-well plates and cultured. Wells were scored as growth or no growth of colonies. LTC-IC frequency was calculated with L-Calc software (StemCell Technologies).

Retroviral transduction of 32Dcl3 cells and differentiation assay

The murine myeloid progenitor 32Dcl3 cells were infected with retrovirus as previously described.[36]

Mouse BMT

Mouse BMT was performed as described previously.[22] Bone marrow (BM) mononuclear cells were isolated from C57BL/6 (Ly-5.1) donor mice, and after stimulation with SCF, FLT-3 ligand, IL-6, and TPO (R&D Systems), the cells were transduced with retrovirus constructs. Then, 3×10^5 to 5×10^5 of the nonsorted cells were injected into sublethally γ-irradiated Ly-5.2 recipient mice. These studies were approved by the Animal Care Committee of the Institute of Medical Science at the University of Tokyo.

Flow cytometry

Human cells were stained with the indicated phycoerythrin (PE) or allophycocyanin–conjugated antibodies (BD). For the cell cycle analysis, the cells were stained with allophycocyanin BrdU Flow Kit (BD) or Hoechst 33342 (BD). Flow cytometry analysis was performed on a FACSCalibur (BD) or FACS Aria, and data were analyzed using CELLQuest. Mouse cells were stained with the indicated PE-conjugated antibodies (eBioscience) and analyzed using FACSCalibur equipped with FlowJo Version 7.2.4 software (TreeStar). Annexin V staining was carried out with the PE Annexin V Apoptosis Detection Kit I (BD).

Immunoblot analysis

Immunoblot analysis was performed as reported previously.[12] The primary antibodies used in this study were anti–FLAG M2 (Sigma-Aldrich), anti-Bmi1 (Upstate, Lake Placid, NY; or #05-637, Millipore), anti–β-actin (Santa Cruz), and anti–α-tubulin (Sigma-Aldrich) monoclonal antibodies.

Statistical analysis

For comparison of 2 independent samples, normally distributed variables were compared by the Student *t* test, and nonnormally distributed variables by the Mann-Whitney *U* test. For multiple pairwise comparisons, the data were analyzed by 1-way analysis of variance followed by Dunnett's multiple comparison test, or differences between individual groups were estimated using the Steel-Dwass test. Survival curves were estimated by the Kaplan-

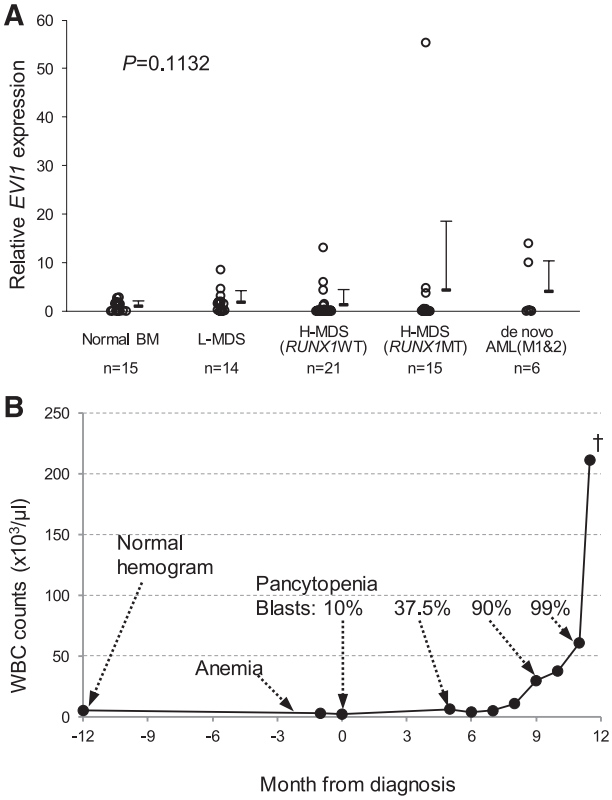

Figure 1. *EVI1* overexpression collaborates with *RUNX1* mutations in human MDSs. (A) *EVI1* expression levels by qRT-PCR in $CD34^+$ cells of clinical samples. Relative *EVI1* expression was calculated as the ratio of *EVI1* to *GAPDH* expression. RNA from normal BM $CD34^+$ cells served as a control, and the RNA level was defined as 1. Data are expressed as mean ± standard deviation (SD). L-MDS, lower-risk MDS; H-MDS, higher-risk MDS; MT, mutation. (B) White blood cell (WBC) count and clinical course of a patient with high *EVI1* expression. A 78-year-old male showed pancytopenia and blast cells in peripheral blood. BM examination showed hypocellular marrow with multilineage dysplasia and 16.5% of blast cells. Cytogenetic analysis showed 45,XY,add(3)(q13.2),-7. He was diagnosed with refractory anemia with excess blasts (RAEB-2) and received chemotherapy. However, his condition progressed to BM failure after chemotherapy and repeated severe infection. The blast population continued to increase gradually. Eight months after diagnosis, his WBC count started to increase, and he died with uncontrollable blast expansion 11.5 months after diagnosis.

Meier analysis and compared using the log-rank test. $P < .05$ was considered statistically significant.

Results

RUNX1 D171 amino acid is the most frequent target of mutations

We analyzed *RUNX1* mutations in various myeloid neoplasms, mostly MDSs and MDS-related AML including therapy-related cases. We found that 107 patients had *RUNX1* mutations, which were shown to be distributed throughout the full length of the RUNX1 protein (supplemental Table 1; see the *Blood* Web site). Replacement of the D171 amino acid (D171N and D171G) was the most frequent target of mutation in the *RUNX1* gene, which was detected in 8 (7.5%) patients. The D171 residue resides in the RHD and is one of the critical amino acid residues that directly contact DNA; however, small changes in the RHD do not influence the ability to bind core binding factor β.[20,21] Moreover, the carboxyl-terminal (C-terminal) region including the transactivation/repression domains is preserved in the mutations (supplemental Figure 1A), contrary to that in truncation-type mutations. Replacement or small in-frame insertions/deletions at or around critical amino acid residues involved in DNA binding were also detected, and 41.6% of the *RUNX1* mutations (45 of 107) had impaired DNA-binding but intact C-terminal transactivation/repression domains. The D171N mutant was localized to the nucleus (supplemental Figure 1B) and showed a loss of normal RUNX1 *trans*-activation potential for the macrophage-CSF receptor (supplemental Figure 1C). Furthermore, the mutant displayed a dominant-negative type of *trans*-activation suppression (supplemental Figure 1D), suggesting that the mutant may have some oncogenic potential in addition to the loss of normal RUNX1 function.

EVI1 overexpression collaborates with RUNX1 mutation in human MDSs

Because collaboration between *RUNX1* mutations and *Evi1* overexpression has been shown in a mouse BMT model,[22] we first checked *EVI1* expression levels in selected $CD34^+$ cells from MDS patients. Most of the examined patients showed very low *EVI1* expression (Figure 1A). However, 1 patient whose initial diagnosis was MDS with D171G mutation displayed an extremely high expression level of *EVI1*. The clinical course of the patient was unique in that a steep increase in blast cells was followed by a relatively short MDS period (Figure 1B), which was similar to that in the mouse BMT model.[22] Thus, expression of *EVI1* is generally not high in MDS patients. Then, we set out to elucidate the collaborating genes with *RUNX1* mutations in other patients.

Overexpression of D171N promotes inhibition of differentiation and increase in self-renewal capacity in human $CD34^+$ cells

To clarify the biological functions of the RUNX1 mutants and to identify their collaborating genes in hematopoietic stem/progenitor cells, we transduced a RUNX1 mutant into human $CD34^+$ cells to avoid the effect of *Evi1* overexpression. The D171N mutant, which was produced by a 1-bp replacement in exon 5, was transduced into $CD34^+$ cells from human CBs (Figure 2A). The efficiency of transduction was ~30% to 60% (Figure 2B), and RUNX1 expression was confirmed by Western blotting (Figure 2C).

To examine the effect of RUNX1 expression on cell differentiation, we performed CFC assay by plating sorted cells in methylcellulose medium. The number of burst-forming unit–erythroid (BFU-E) colonies was significantly decreased in both WT- and D171N-transduced cells, whereas the number of colony-forming unit GM (CFU-GM) colonies was not significantly different (Figure 2D). On the other hand, the individual BFU-E colonies in the WT plates and individual CFU-GM colonies in the D171N plates were larger in size (Figure 2E), in addition to the presence of significantly more growing cells as compared with the control (Figure 2F). Glycophorin A (GPA^+) erythroid cells were dominant in the WT group, whereas most of the D171N-transduced cells expressed myeloid lineage markers (Figure 2G). To determine whether D171N has a self-renewal advantage, we performed replating CFC assay. The plates of the D171N mutant contained approximately half the total number of colonies as the pMXs.IG plates in the first assay, whereas total cell numbers were comparable between the D171N and pMXs.IG plates (Figure 2H). Unlike pMXs.IG and WT, D171N showed replating capacity for 3 replatings. To confirm the presence of progenitors with long-term self-renewal capabilities, LTC-IC assay was conducted. Cells transduced with D171N showed a drastic increase in the number of colonies (Figure 2I).

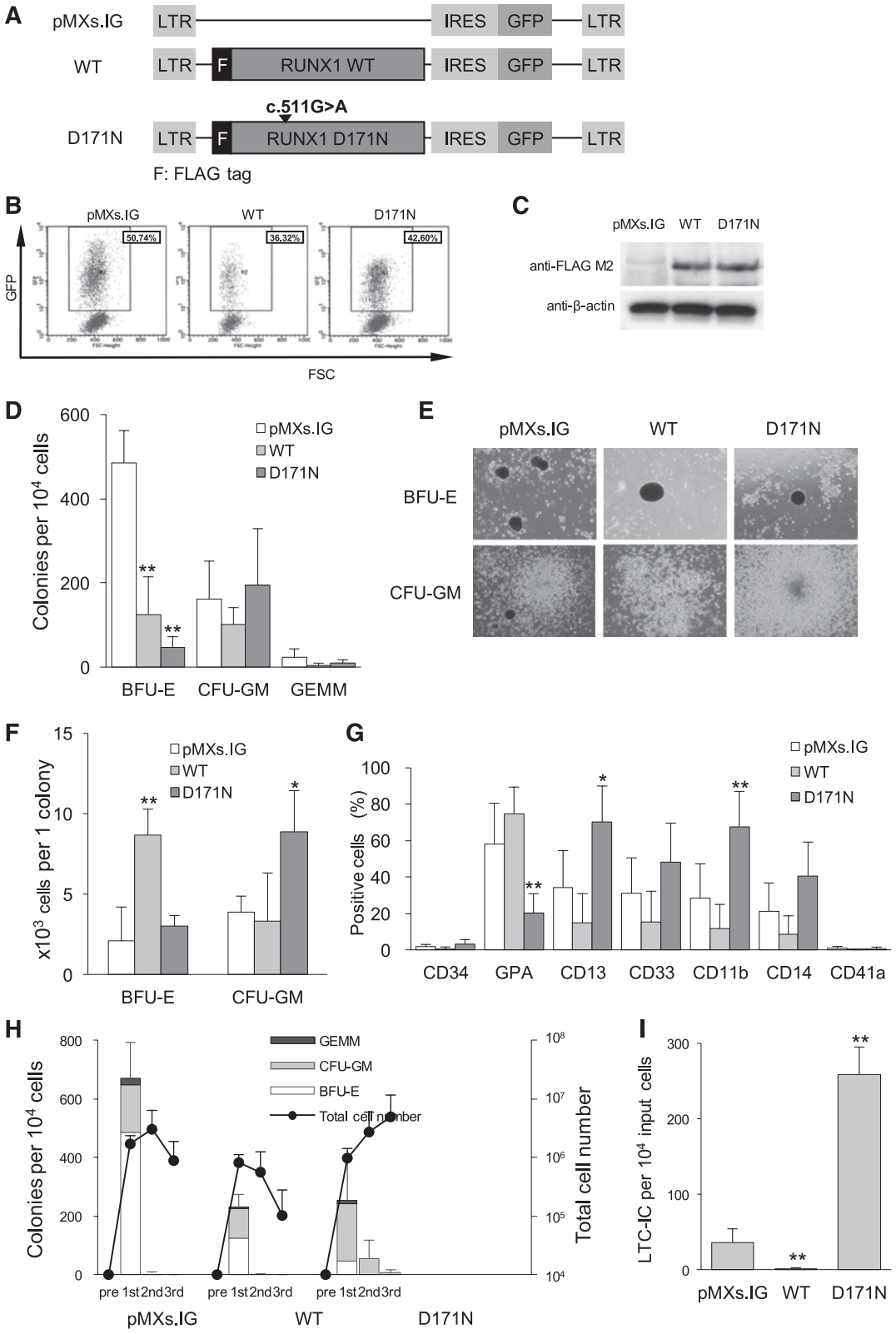

Figure 2. Overexpression of D171N promotes inhibition of differentiation and increase in self-renewal capacity. (A) Pictogram of pMXs.IG retroviral constructs of the FLAG-tagged RUNX1 WT and the D171N mutant (D171N). The difference in cDNA sequence of the mutant from the WT is indicated by an arrowhead. LTR, long terminal repeat. (B) Human CD34$^+$ CB cells were transduced with the indicated vector. A typical flow cytometry profile of cells retrovirally transduced with pMXs.IG, WT, or D171N shows the transduction efficiency. The GFP$^+$ cells shown within the gate were collected. (C) Anti-FLAG immunoblotting of sorted GFP$^+$ cells confirmed the expression of FLAG-tagged RUNX1 proteins. Anti–β-actin antibody was used as control. (D-H) Ten thousand cells were plated in methylcellulose culture dishes. GEMM, colony-forming unit–granulocyte, erythroid, macrophage, megalocyte. Data are expressed as mean ± SD of 6 independent experiments and compared with control (pMXs.IG). *$P < .05$; **$P < .01$. (D) Colony numbers were counted after 14 days. (E) Photomicrographs (×40) of representative colonies found in the plates with an IX71 microscope and a DP12 camera (Olympus). (F) The cell number per colony was calculated by total GPA$^+$ cells/total BFU-E colonies and total CD13$^+$ cells/total CFU-GM colonies. (G) GFP$^+$ cells were analyzed by flow cytometry for the indicated surface markers. (H) Colony number and cell proliferation fold in CFC replating assay. (I) LTC-IC assay in bulk was carried out in duplicate, and the average number of LTC-IC per 10 000 original input cells and SD of 4 independent experiments are indicated. **$P < .01$.

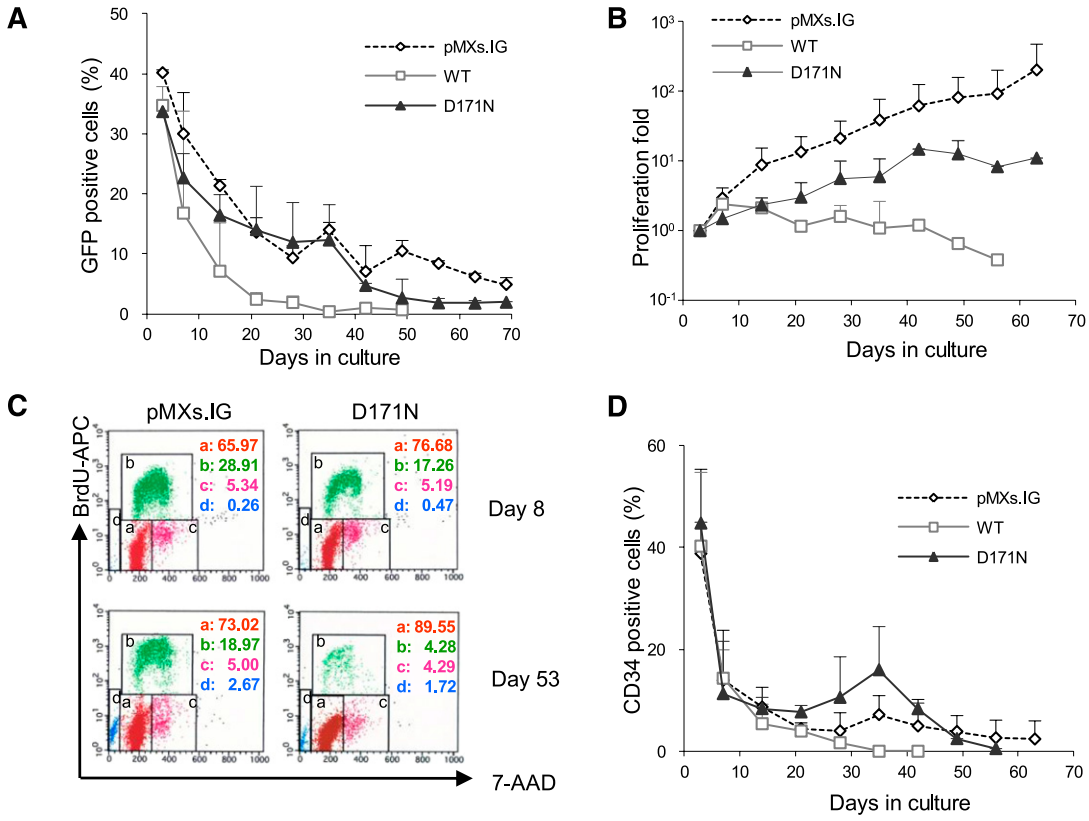

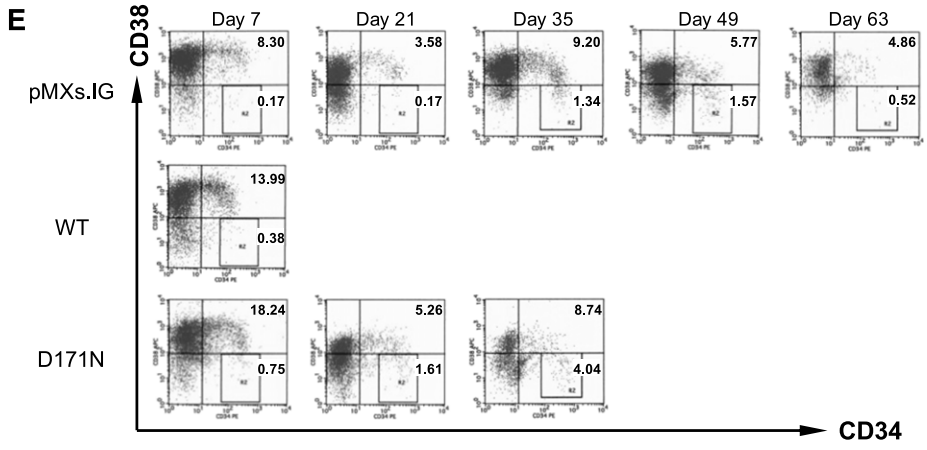

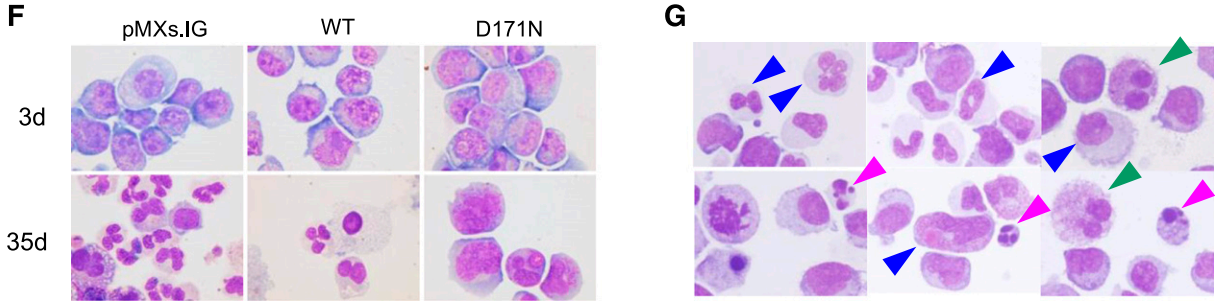

Figure 3. D171N-transduced cells lack long-term proliferation ability. Human CD34$^+$ CB cells were transduced with the indicated vectors and cultured in complete cytokine medium (without IL-3 and IL-6). To examine proliferation ability of each transduced cell type, the cells were sorted for GFP expression and cultured in complete cytokine medium. Four independent experiments were performed, and the error bars represent the SD. (A) Proliferation curve of GFP$^+$ RUNX1-transduced or control (empty vector-transduced) cells, nonsorted. (B) Growth patterns of the GFP-sorted transduced cells displayed as proliferation fold originating from 10° just after sorting. (C) Representative quantitative cell cycle analysis allowed the discrimination of cell subsets that were undergoing G0/G1 (a), S (b), or G2 + M (c) phases of the cell cycle, or apoptosis (d). (D) Percentage of CD34$^+$ cells was determined by flow cytometry. (E) Representative CD34/CD38 expression pattern in long-term culture. (F) Images of Wright-Giemsa–stained cytospins on days 3 and 35 obtained with a BX51 microscope and a DP12 camera (Olympus); original magnification ×1000. (G) Morphologic abnormalities observed in Wright-Giemsa–stained cytospins of the D171N cells on day 35 in culture, myeloid, erythroid, and megakaryocytic cells with dysplasia are indicated by blue, pink, and green arrows, respectively, as captured with a BX51 microscope and a DP12 camera (Olympus); original magnification ×1000.

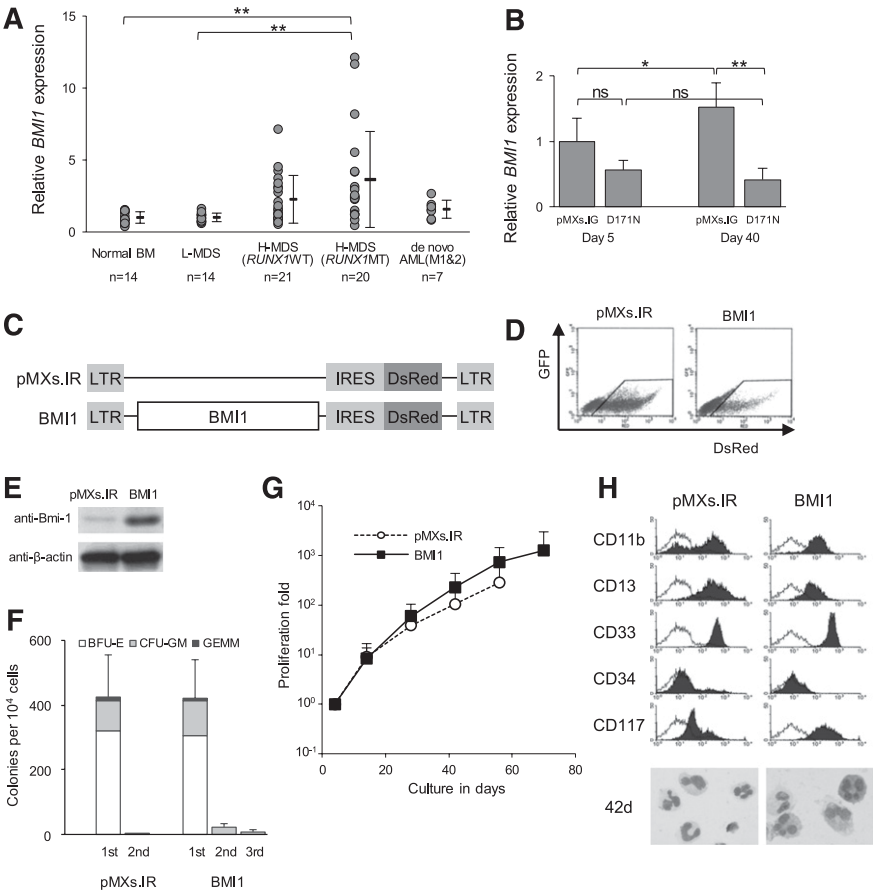

Figure 4. BMI1 expression pattern in human CD34$^+$ cells and enforced BMI1 expression in human CD34$^+$ cells. (A) BMI1 expression levels in CD34$^+$ cells of clinical samples. Relative BMI1 expression was measured by triplicated qRT-PCR and calculated as the ratio of BMI1 to GAPDH expression. Data are also expressed as mean ± SD of each patient group. $^{**}P < .01$. (B) BMI1 expression in transduced CD34$^+$ cells was confirmed by qRT-PCR. CD34$^+$ cells were repurified from GFP$^+$ sorted cells after 5 and 40 days of culture in complete cytokine medium. Bar chart represents the mean ± SD of 3 independent experiments. RNA from pMXs.IG-transduced cells on day 5 served as a control, and the RNA level was defined as 1. $^*P < .05$; $^{**}P < .01$. (C) pMXs.IRES-DsRed-Express (pMXs.IR) retroviral construct for the expression of BMI1. (D) Representative flow cytometry profile of cells retrovirally transduced with pMXs.IR or BMI1 shows the transduction efficiency. The DsRed$^+$ cells shown within the gate were collected. (E) Expression of BMI1 was confirmed by Western blotting using anti-Bmi1 antibody. Anti–β-actin antibody was used as the control. (F) Human CD34$^+$ cells transduced with the indicated vector and sorted for DsRed expression were analyzed by CFC replating assay. Ten thousand cells were plated in methylcellulose culture dishes. Data are expressed as mean ± SD of 3 independent experiments. (G) Growth pattern of the transduced cells cultured in complete cytokine medium displayed as proliferation fold originating from 10^0 just after sorting. The error bars represent the SD from 4 independent experiments. (H) The expression pattern of surface markers as shown by a typical flow cytometry profile, and Wright-Giemsa–stained cytospins of the DsRed$^+$ cells on day 42 culture in complete cytokine medium as captured with a BX51 microscope and a DP12 camera (Olympus); original magnification ×1000.

D171N-transduced cells lack long-term proliferation ability in human CD34$^+$ cells

To determine proliferative and survival advantages of RUNX1-mutated cells, transduced nonsorted human CD34$^+$ cells were cultured in liquid medium (Figure 3A). The percentage of GFP-expressing cells in the WT, D171N, and pMXs.IG-transduced control cultures gradually decreased over time in culture. For further evaluation of the proliferation ability of the transduced cells, we sorted GFP$^+$ cells and performed long-term culture. The WT-transduced cells hardly proliferated, whereas the D171N-transduced cells proliferated slightly, exhibiting lower proliferation ability than pMXs.IG cells (Figure 3B). These results indicate that the D171N cells have no proliferation ability. To determine whether these differences were due to increased apoptosis or cell cycle inhibition, we confirmed by cell cycle analysis. On day 53 when the D171N cells stopped proliferating, most of the cells accumulated in the G1 phase (Figure 3C). The percentage of CD34$^+$ cells among the D171N cell population increased slightly but gradually decreased with a maximum at approximately day 35 (Figure 3D). At this point, although the percentage of CD34$^+$/CD38$^+$ cells within the D171N cell population did not increase in comparison with the pMXs.IG group, the percentage of CD34$^+$/CD38$^-$ cells increased to a maximum at ~4% (Figure 3E). On day 35, a vast majority of the pMXs.IG cells and all the WT cells terminally differentiated into mature myeloid cells and monocytes, whereas the D171N cells contained a large number of immature cells (Figure 3F). The cells transduced with the D171N mutant displayed morphologic abnormalities in all 3 hematopoietic lineages (Figure 3G). These findings indicate that RUNX1 mutations probably give rise to the multilineage dysplasia of hematopoietic cells with increase in the number of blasts, which is the main characteristic of MDSs. However, the D171N-transduced cells did not expand in liquid media. Furthermore, the D171N mutant abrogated engraftment potential of human stem/progenitor cells in NOD/Shi-scid, IL2Rγc^{null} (NOG) mice[37] (supplemental Table 2). Thus, it is suspected that the mutant requires additional gene alterations for the development of MDSs.

BMI1 is overexpressed in CD34$^+$ cells from MDS patients with RUNX1 mutations, whereas it is repressed in D171N-transduced human CD34$^+$ cells

We focused on *BMI1* as a candidate of the additional partner gene alterations because this gene is known to be overexpressed in some MDS patients. *BMI1* expression levels were analyzed in selected CD34$^+$ cells from MDS patients (Figure 4A). Patients with *RUNX1* mutations displayed a significantly higher expression level of *BMI1* compared with normal control and lower-risk MDS patients, and 14 of 20 (70%) of the RUNX1-mutated patients showed *BMI1* overexpression that exceeded the range of normal control, as opposed to only 1 with *EVI1* overexpression. Next, we examined *BMI1* expression levels in the D171N-transduced CD34$^+$ cells over a time course. Unexpectedly, the cells with D171N mutation showed a lower expression level of *BMI1*, especially during a long culture period (Figure 4B). These results indicate that the high *BMI1* expression in patients with RUNX1 mutations is not induced by direct effects of the mutations, but rather, the RUNX1-mutated cells may require the acquisition of *BMI1* overexpression for the development of MDSs. To confirm the effects of additional *BMI1* overexpression on D171N-transduced cells, we antecedently analyzed BMI1-transduced CD34$^+$ cells.

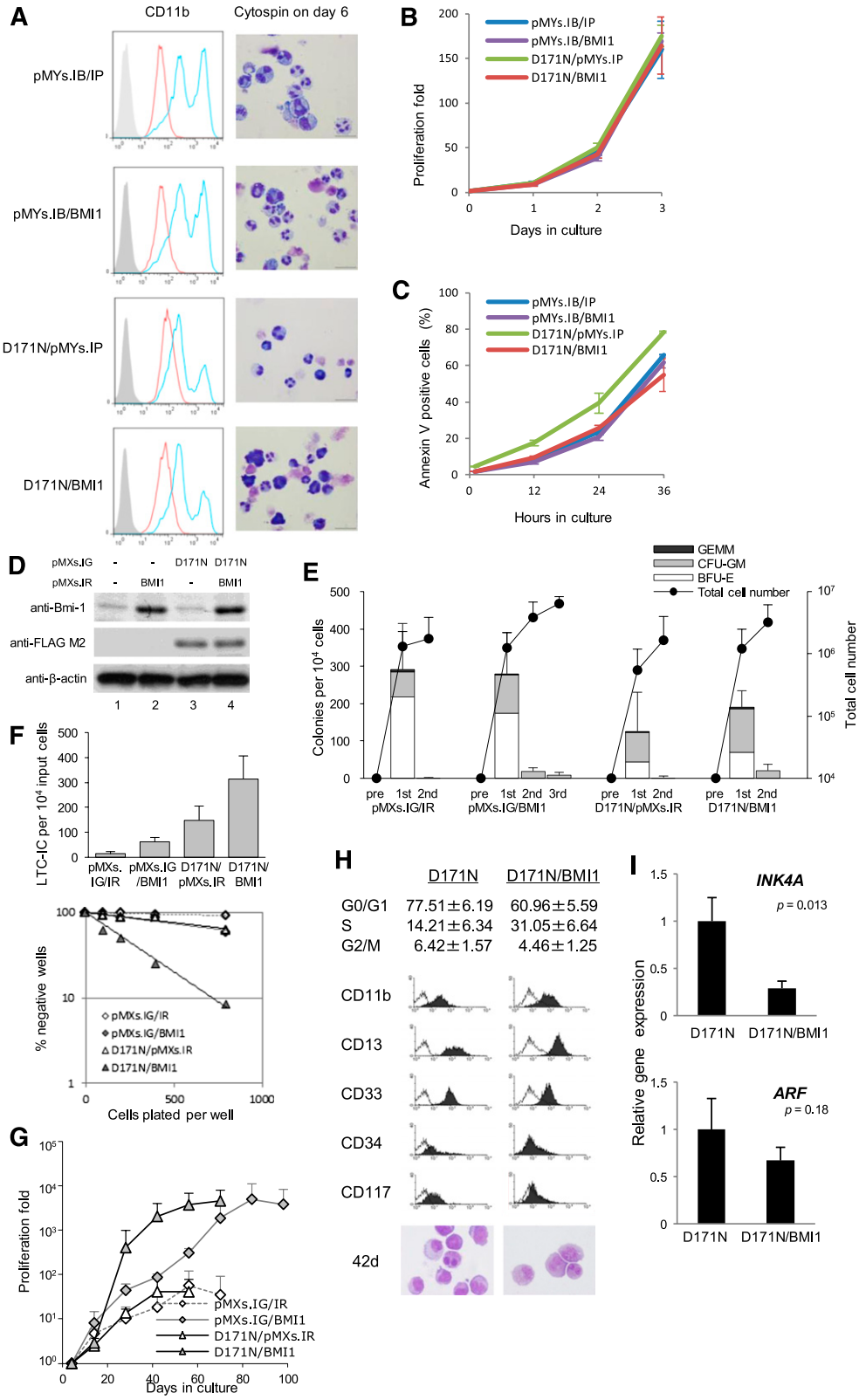

Figure 5. The effect of double expression of D171N and BMI1. (A-C) IL-3–dependent 32Dcl3 cells were stably transduced with pMYs.IP/IB, pMYs.IP/BMI1, D171N/pMYs.IB, or D171N/BMI1. Before the assay for proliferation and apoptosis, the transduced 32Dcl3 cells were subjected to drug selection with 1 μg/mL puromycin and 10 μg/mL blasticidin. (A) G-CSF–induced differentiation assay in indicated 32Dcl3 transfectants. Surface expression of CD11b after incubation for 6 days in the presence of 1 ng/mL IL-3 (red histograms) or 50 ng/mL G-CSF (blue histograms) was analyzed by flow cytometry. The result of control staining is shown as a filled histogram. Data are representative of 2 independent experiments. The cells cultured with G-CSF for 6 days were assessed by Giemsa staining. Images were obtained with a BX51 microscope and a DP12 camera (Olympus); objective lens, UplanFl (Olympus); original magnification ×1000. (B) Growth curve of the transduced 32Dcl3 cells cultured in the presence of 1 ng/mL of IL-3. Data are expressed as mean ± SD of 3 independent experiments. (C) Annexin V positivity in the transduced 32Dcl3 cells cultured without IL-3. Data are expressed as mean ± SD of 3 independent experiments. (D-G) Human $CD34^+$ cells were precultured for 3 to 4 days in expansion medium and transduced with both GFP-tagged D171N and

Enforced BMI1 expression shows no leukemogenic ability in human CD34$^+$ cells

To evaluate the biological significance of BMI1 overexpression in stem/progenitor cells, BMI1 was cloned into a retrovirus vector (Figure 4C) and transduced into CD34$^+$ cells (Figure 4D). BMI1 was endogenously expressed in cells transduced with pMXs.IR, whereas a strong upregulation of this protein was observed in the BMI1-transduced cells (Figure 4E). The number of colonies of the BMI1-transduced CD34$^+$ cells was almost equal to that of the pMXs.IR-transduced cells, whereas the replating efficiency of the BMI1 cells was slightly increased (Figure 4F). The BMI1-transduced cells exhibited greater proliferation than the pMXs.IR-transduced cells (Figure 4G), but the cells proliferated with myeloid terminal differentiation without dysplasia or increase in CD34$^+$ cells (Figure 4H). Thus, BMI1-overexpressed cells showed a slight increase in self-renewal capacity and an increase in proliferation ability. However, BMI1 did not block differentiation at all. Overexpression of BMI1 may have limited proliferation ability without differentiation inhibition, suggesting that BMI1 alone does not have enough potential for MDS genesis.

These results raised the possibility that BMI1 may be overexpressed by additional molecular abnormalities and may work as a proliferative activator in the stem/progenitor cells with RUNX1 mutations. Because the D171N mutation itself was not proliferogenic, our next investigation was undertaken to determine whether BMI1 is required for leukemogenesis in the D171N-mutated cells.

BMI1 overexpression confers survival advantage but does not inhibit G-CSF–induced differentiation of 32D cells

To confirm the collaboration of D171N with BMI1, we first transduced both the D171N mutant and BMI1 into 32Dcl3 cells. The 32Dcl3 cells were transduced with pMYs.IP/IB, pMYs.IP/BMI1, D171N/pMYs.IB, or D171N/BMI1, and the infected cells were subjected to drug selection by puromycin and blasticidin. G-CSF treatment induced terminal differentiation of 32Dcl3 cells transduced with pMYs.IP/IB, as indicated by the appearance of polymorphonucleated neutrophils and upregulation of CD11b on the surface, and pMYs.IP/BMI1-transduced cells were also terminally differentiated as well (Figure 5A). However, the differentiation was weakly inhibited by D171N/pMYs.IB, and D171N/BMI1 showed no additional effect on differentiation compared with D171N/pMYs.IB (Figure 5A), indicating that BMI1 did not block differentiation at all. Growth rate was comparable among the indicated transfectants after 3 days of culture with the presence of IL-3 (Figure 5B). However, annexin V positivity in the D171N/BMI1-transduced cells was at the same level as that in pMYs.IG/IB- or pMYs.IP/BMI1-transduced cells, and it was significantly lower than that in D171N/pMYs.IB-transduced cells after 36 hours of culture without IL-3 (Figure 5C). These data raised the possibility that BMI1 may add some survival effects to D171N-transduced cells.

Double transduction of D171N and BMI1 into human CD34$^+$ cells leads to proliferation with differentiation

To investigate whether BMI1 can add a growth advantage to RUNX1-mutated cells, we performed simultaneous double transduction of the D171N mutant with BMI1 into human CD34$^+$ cells. Human CB CD34$^+$ cells were transduced with pMXs.IG/IR, pMXs.IG/BMI1, D171N/pMXs.IR, or D171N/BMI1. BMI1 was endogenously expressed in cells transduced with pMXs.IG/IR or D171N/pMXs.IR, whereas a strong upregulation of this protein was observed in the BMI1-transduced cells (Figure 5D). In the CFC replating assay, all of the double-transduced cells formed fewer colonies than single-transduced cells (Figure 5E, compared with Figures 2H and 4F). Both colony number and replating ability were altered by the double transduction of D171N and BMI1 compared with D171N/pMXs.IR-transduced cells. The presence of stem/progenitor cells with long-term self-renewal capabilities was confirmed by the LTC-IC assay. In both limiting dilution and bulk assays, increased stem/progenitor cell frequencies were observed in D171N/BMI1-transduced cells (Figure 5F). In addition, a dramatic change was observed in the liquid culture. Double-transduced cells with pMXs.IG/IR or D171N/pMXs.IR hardly proliferated in the long-term culture medium, and their proliferation folds were <100 (Figure 5G). However, double-transduced cells containing BMI1 exhibited an altered effect on cell proliferation. In particular, the D171N/BMI1 double-transduced cells spontaneously started to proliferate at approximately day 20, a phenomenon that was earlier and greater than the cells with pMXs.IG/BMI1. The D171N/BMI1 cells markedly grew until day 70, resulting in the same proliferation ability when compared with pMXs.IG/BMI1-transduced cells (Figure 5G). Thus, the D171N/BMI1-transduced cells had a strong growth advantage compared with the D171N/pMXs.IR-transduced cells. The BMI1 double-transduced cells showed an increase in S phase; however, the cells did not harbor an expansion of a population of CD34$^+$ or blast cells, and most of the cells differentiated to various stages of myeloid cells with dysplasia (Figure 5H). These results indicate that BMI1 overexpression confers proliferation ability with differentiation to D171N-mutated cells. To assess the impact of BMI1 on the proliferation and survival of the progenitor cells, we analyzed the effect of *BMI1* expression on *INK4A/ARF* (*p16/p14*) locus expression in the CD34$^+$ cells. *INK4A/ARF* expression was downregulated by BMI1 (Figure 5I), which may have contributed to the proliferation and survival of D171N-transduced cells. Significant enrichments of BMI1 on *Ink4a/Arf* (*p16/p19*) promoter regions were detected in both BMI1-transduced 32D cells and BMI1/D171N-transduced 32D cells, but not on the β-actin promoter region (supplemental Figure 2A). A physical association in vivo between BMI1 and D171N was observed in 293T cells, which was comparable to that between BMI1 and WT RUNX1 (supplemental Figure 2B).

INK4A/ARF expression levels were also lower in MDS patients with RUNX1 mutations than in those without mutations in this gene (supplemental Figure 3A). To clarify the role of

Figure 5 (continued) DsRed-tagged BMI1. After 3 to 4 days, GFP$^+$/DsRed$^+$ cells were purified by sorting. The cells were cultured in methylcellulose or long-term culture medium. (D) Expression of BMI1 and RUNX1-D171N were confirmed by Western blotting using anti-Bmi1 and anti–FLAG M2 antibodies, respectively. Anti–β-actin antibody was used as control. (E) Double-transduced cells were analyzed by CFC replating assay. Data are expressed as mean ± SD from 4 independent experiments. (F) LTC-IC assay in bulk and limiting dilution was carried out. (G) Growth patterns of the transduced cells cultured in long-term culture medium displayed as proliferation fold. The error bars represent the SD from 4 independent experiments. The growth profiles of all cells with double transduction of GFP (empty or D171N) and DsRed (empty or BMI1) vectors are shown. (H) Cell cycle analysis and the expression pattern of surface markers as shown by a typical flow cytometry profile, and Wright-Giemsa–stained cytospins of D171N- and D171N/BMI1-transduced cells on day 42 as captured with a BX51 microscope and a DP12 camera (Olympus); original magnification ×1000. (I) *INK4A/ARF* (*p16/p14*) expression levels in D171N- and D171N/BMI1-transduced cells on day 42. Relative gene expression was measured by qRT-PCR performed in triplicate and calculated as the ratio of *INK4A/ARF* to *GAPDH* expression.

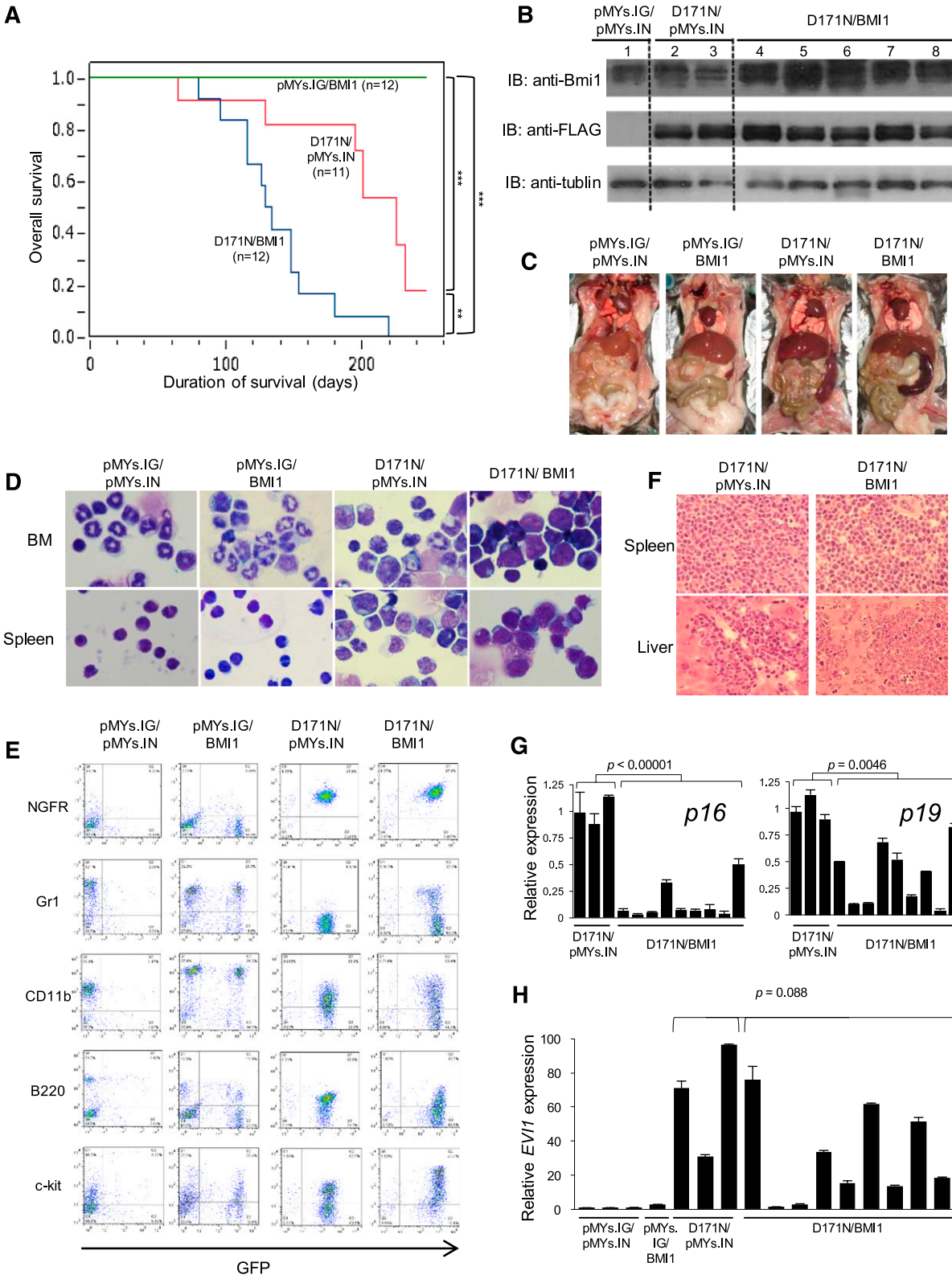

Figure 6. The effect of double expression of D171N and BMI1 in a mouse BMT model. (A) Kaplan-Meier analysis of the survival of mice that received transplants of BM cells transduced with pMYs.IG/BMI1 (n = 12, green line), D171N/pMYs.IN (n = 11, red line), or D171N/BMI1 (n = 12, blue line). *P* values were calculated using log-rank test. (B) Expression of RUNX1-D171N and BMI1 in BM cells derived from the BMT mice transduced with pMYs.IG/IN (lane 1), D171N/pMYs.IN (lanes 2, 3), or D171N/BMI1 (lanes 4-8). Cell lysates were immunoblotted with anti-Bmi1, anti–FLAG M2, or anti-tubulin antibody as control. Data are representative of 3 independent experiments. (C) Macroscopic findings of euthanized mice transplanted with BM cells transduced with the indicated construct. A representative photograph is shown. Mice with D171N/pMYs.IN or D171N/BMI1 died of MDS/AML with marked splenomegaly (right 2 panels), although mice with pMYs.IG/IN or pMYs.IG/BMI1 remained healthy without any organomegaly 8 months after BMT (left 2 panels). (D) Cytospin preparations of BM and spleen cells derived from indicated mice were stained with Giemsa. A representative photograph is shown. Images were obtained with a BX51 microscope and a DP12 camera (Olympus); objective lens, UplanFl (Olympus); original magnification ×1000. (E) Flow cytometric analysis of BM cells derived from each transduced mouse. In pMYs.IG/IN and pMYs.IG/BMI1, apparently healthy mice were euthanized for analysis of BM cells 8 months after BMT.

Table 1. Characteristics of AML mice caused by expression of D171N and BMI1

Characteristics	pMYs.IG/pMYs.IN (n = 3)	D171N/pMYs.IN (n = 5)	D171N/BMI1 (n = 10)
WBCs (/μL)	18 550 ± 1786	129 100 ± 68 089	70 838 ± 16 353
Hb (g/dL)	14.8 ± 0.4	7.3 ± 2.5	7.7 ± 2.3
PLTs ($\times 10^3$/μL)	291 ± 67	246 ± 80	134 ± 75
MCV (fL)	46.7 ± 0.6	53.6 ± 3.9	51.9 ± 9.3
BM count ($\times 10^7$ cells)	2.70 ± 0.78	7.05 ± 1.67	4.83 ± 1.14
Myeloblasts in BM (%)	1.8 ± 1.0	34.5 ± 16.0	59.6 ± 8.2
Liver weight (mg)	1668 ± 129	2008 ± 482	2015 ± 527
Spleen weight (mg)	98 ± 12	605 ± 242	531 ± 185

Averages and standard deviations are shown. BM cells were isolated from both tibias and femurs.

Hb, hemoglobin; MCV, mean corpuscular volume; PLTs, platelets.

micro RNAs (miRNAs) associated with BMI1 and polycomb-repressive complex (PRC) 1/2 in the patients with RUNX1 mutations, we analyzed miRNA levels in $CD34^+$ cells from MDS patients; however, no remarkable difference was detected between $CD34^+$ cells from patients and normal BM (supplemental Figure 3B). Furthermore, we analyzed the effects of BMI1 knockdown by short hairpin RNA in the $CD34^+$ cells from MDS/AML patients with RUNX1 mutations and high BMI1 expression. BMI1 knockdown resulted in impaired cell proliferation on MS5 stromal cells (supplemental Figure 3C). These results indicate that expansion of RUNX1-mutated $CD34^+$ cells depends on BMI1 expression, which coincides with repression of the cell cycle regulators INK4A/ARF.

Collaboration of the D171N mutant and BMI1 in a mouse BMT model

Nevertheless, even the D171N/BMI1-transduced human $CD34^+$ cells did not develop MDS/AML in NOG mice (supplemental Table 2). Therefore, to confirm the collaboration of BMI1 overexpression with the D171N mutant in vivo, we performed mouse BMT using BM cells transduced with both D171N and BMI1. We previously reported that most of the mice that received D171N-transduced BM cells died of MDS/AML, and collaboration between D171N and Evi1 overexpression was confirmed in a BMT model where coexpression of D171N and Evi1 induced MDS/AML with much shorter latencies.[22] To investigate whether high expression of BMI1 can also collaborate with D171N, Ly-5.1 murine BM mononuclear cells were infected with retrovirus harboring pMYs.IG/IN, pMYs.IG/BMI1, D171N/pMYs.IN, or D171N/BMI1. The efficiency of retrovirus infection was 35% to 45% of $GFP^+/NGFR^+$ cells (supplemental Figure 4A; supplemental Table 3), and nonsorted cells were transplanted into sublethally irradiated syngeneic Ly-5.2 mice. Each cell population was successfully engrafted (supplemental Figure 4B), and in time, the proportion of $GFP^+/NGFR^+$ cells gradually increased in the mice that were transplanted with D171N/BMI1-transduced cells (supplemental Figure 4C).

Mice that received transplants of pMYs.IG/BMI1-transduced cells remained healthy over the observation period (n = 12/12), as well as those that were transplanted with pMYs.IG/IN-transduced cells (n = 4/4). Most of the mice that received transplants of D171N/pMYs.IN-transduced cells developed MDS/AML mainly 6 to 8 months after transplantation (n = 6/11, $P < .0001$, Figure 6A), as observed in the previous report.[22] Of note, mice that received transplants of BM cells expressing D171N/BMI1 developed MDS/AML with significantly shorter latencies (mainly 3 to 5 months) compared with the D171N/pMYs.IN group (n = 12/12, $P = .001$, Figure 6A). Expression of the transduced D171N and BMI1 was confirmed by Western blot analysis, and endogenous Bmi1 expression could be detected in the D171N/pMYs.IN cohort (Figure 6B). Morbid mice with D171N/pMYs.IN or D171N/BMI1 exhibited similar phenotypes, characterized by leukocytosis, anemia, and marked splenomegaly, whereas the mice with pMYs.IG/BMI1 or pMYs.IG/IN, euthanized 8 months after BMT, showed none of these phenotypes (Table 1 and Figure 6C). In the leukemic mice with D171N/pMYs.IN or D171N/BMI1, BM and spleen were occupied by immature myeloid cells including myeloid blasts (Figure 6D). More myeloblasts in BM were observed in D171N/BMI1 mice than in D171N/pMYs.IN ones (Table 1). The leukemic cells displayed similar morphologic abnormalities and surface markers: $GFP^+/NGFR^+$ leukemic cells were $CD11b^{low\ to\ high}$, $Gr\text{-}1^{low}$, $B220^{low}$, and $c\text{-}kit^{low\ to\ high}$ (Figure 6E; supplemental Figure 4D; supplemental Table 2), although the expression level of c-kit tended to be higher in the D171N/BMI1 cohort than that in the D171N/pMYs.IN group. The normal structure of the spleen was completely destroyed with massive blast and immature myeloid cell infiltration, and these cells also invaded into the hepatic portal areas in the liver (Figure 6F). Meanwhile, $GFP^+/NGFR^+$ cells in pMYs.IG/BMI1-induced mice were very few, indicating that pMYs.IG/BMI1-transduced BM cells did not become dominant in vivo (Figure 6E). In addition, myeloid cells showed normal differentiation into segmented cells in the BM, and most of the nucleated cells in the spleen were found to be small lymphocytes as observed in the mice with pMYs.IG/IN (Figure 6D). Collectively, BMI1 overexpression has a strong potential to induce MDS/AML in concert with D171N in a mouse BMT model, although BMI1 overexpression by itself does not result in maturation block or leukemogenesis. Furthermore, *Ink4a/Arf* (*p16/p19*) expression in D171N/BMI1-transduced mice was significantly lower than that in the D171N/pMYs.IN-transduced mice (Figure 6G). However, most of the D171N/BMI1 mice still showed high expression of *Evi1*, which was relatively lower than that in the D171N/pMYs.IN group (Figure 6H). Therefore, *Evi1* overexpression is suspected to play a critical role along with the RUNX1 D171N mutation in the development of MDS/AML in the mouse system.

Stepwise transduction of the D171N mutant and BMI1 leads to MDS-like long-term proliferation in human $CD34^+$ cells

Our results showed that simultaneous transduction of D171N and BMI1 can induce MDS/AML, whereas FPD/AML patients who have congenital RUNX1 mutations develop MDS/AML after decades of latency period. This raises the possibility that additional gene abnormalities occur afterward in the RUNX1-mutated cells for the development of MDSs. To clarify the effect of BMI1 in RUNX1-mutated $CD34^+$ cells, we next performed stepwise transduction of the D171N mutant and BMI1 (Figure 7A).

Figure 6 (continued) The dot plots show staining for NGFR, Gr-1, CD11b, B220, or c-kit as detected with PE vs GFP. (F) Histopathological findings of spleen and liver from mice that died of MDS/AML in the indicated BMT model, as shown by hematoxylin and eosin staining. Images were obtained with a BX51 microscope and a DP12 camera (Olympus) with an UplanFL objective lens (Olympus) and are shown at an original magnification ×400. (G) *Ink4a/Arf* (*p16/p19*) expression levels in BM cells of mice. Relative *p16/p19* expression was measured by qRT-PCR performed in triplicate and calculated as the ratio of *p16/p19* to *Gapdh* expression. (H) *Evi1* expression levels in BM cells of mice. Relative *Evi1* expression was measured by qRT-PCR performed in triplicate and calculated as the ratio of *Evi1* to *Gapdh* expression. RNA from pMYs.IG/pMYs.IN mice served as a control, and the RNA level was defined as 1.

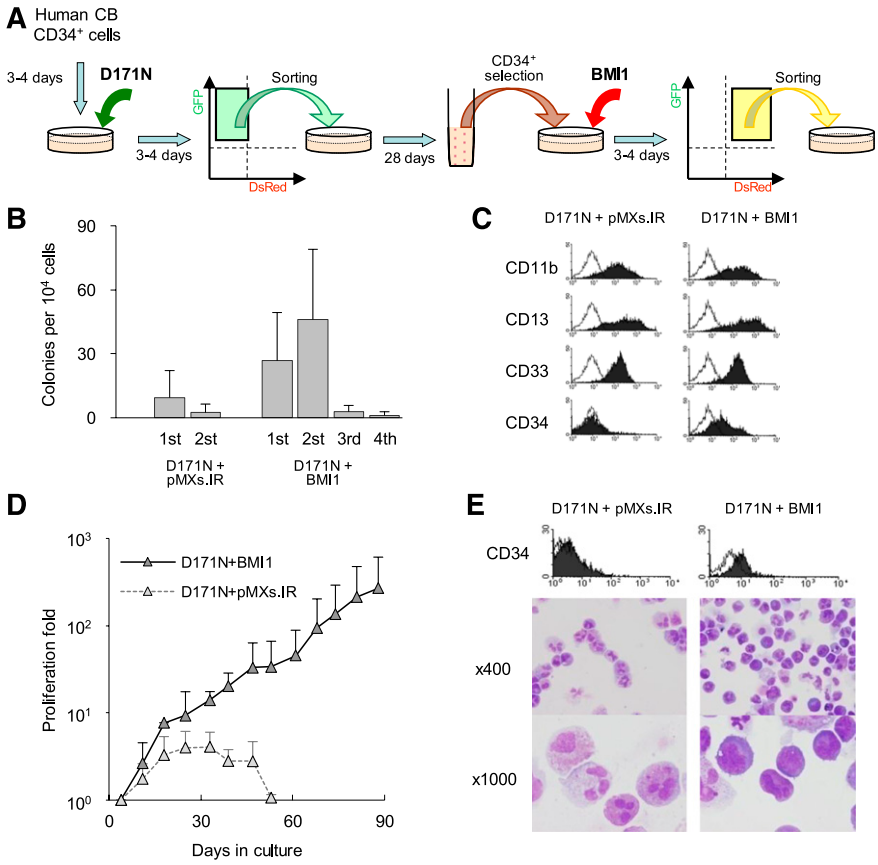

Figure 7. Stepwise transduction of the D171N mutant followed by BMI1 in human CD34$^+$ cells. (A) Human CD34$^+$ cells were precultured for 3 to 4 days in expansion medium and transduced with GFP-tagged D171N-mutant. After 3 or 4 days, GFP$^+$ cells were sorted and cultured in long-term culture medium for 28 days. Then, CD34$^+$ cells were reselected by the CD34 MicroBead Kit again and transduced with DsRed-tagged BMI1. We also transduced the DsRed vector as a control. Finally, 35 days after the D171N transduction, GFP$^+$/DsRed$^+$ cells were sorted and cultured in methylcellulose or long-term culture medium. (B) CFC replating assay in 3 independent experiments. (C) Representative flow cytometry analyses of the first colonies. (D) Proliferation fold in 3 independent experiments. Day 0 was the day of the second (DsRed vectors) transduction. (E) Flow cytometric analysis for CD34 expression, and Wright-Giemsa–stained cytospins on day 39 as captured with a BX51 microscope and a DP12 camera (Olympus) at ×400 and ×1000 original magnifications.

We first transduced D171N into CD34$^+$ cells. Sorted GFP$^+$ cells were cultured for 28 days more, until the percentage of the D171N-transduced CD34$^+$ cells, especially the CD34$^+$/CD38$^-$ population, was maximal (Figure 3D-E). Then, we selected for the CD34$^+$ cells again, followed by BMI1 transduction. GFP$^+$/DsRed$^+$ cells were sorted and cultured in methylcellulose or long-term culture medium. In the CFC assay, pMXs.IR-transduced cells seemed to have very low colony-forming ability, whereas the stepwise BMI1-transduced D171N cells displayed an increase in both colony-forming ability and replating capacity (Figure 7B). Moreover, the CD34$^+$ cell population remained in the stepwise BMI1-transduced D171N cells (Figure 7C). Furthermore, long-term proliferation with a retained CD34$^+$ cell fraction was observed in the stepwise BMI1-transduced D171N cells, and morphologic findings showed myeloid cell dysplasia with increased blast cells (Figure 7D-E). These findings are quite similar to those seen in human patients with higher-risk MDSs. Thus, our results demonstrate that the MDS phenotype could be reproduced in human hematopoietic cells by stepwise transduction of the D171N mutant followed by BMI1.

Discussion

RUNX1 mutations have been detected in nearly 20% patients with higher-risk MDSs. Biochemically, RUNX1 mutants show loss of normal RUNX1 function, and some mutants have dominant-negative *trans*-activation potential similar to leukemogenic chimeras such as CBFβ-MYH11. The biological functions of RUNX1 mutants, which have already been demonstrated using the mouse BMT model, include increase in leukemogenic potential.[22] In this model, however, the retrovirus frequently integrated into the chromosome near the *Evi1* locus, resulting in its high expression. We checked *EVI1* expression levels in MDS patients; however, most of the examined patients showed very low *EVI1* expression, except for only 1 patient with a *RUNX1* mutation, who rapidly progressed from MDS to AML with hyperblastcytosis. Because collaboration between *RUNX1* mutations and *EVI1* overexpression does not appear to be common in MDS patients, we tried to clarify the biological significance of RUNX1 mutants in stem/progenitor cells using human CBs without the effect of *Evi1* overexpression.

The cells transduced with WT RUNX1 quickly differentiated into mature myeloid/monocytoid cells without proliferation in both colony-forming and liquid culture assays. This result suggests that overexpression of WT RUNX1 in stem/progenitor cells promotes terminal differentiation without self-renewal, blocks cell proliferation, and has no oncogenic potential. These data can explain the reduction in WT RUNX1-transduced cells in a mouse BMT model.[22,38] On the other hand, the D171N mutant, the most common mutation in RUNX1 that is caused by only a 1-bp replacement in the RHD, has increased self-renewal capacity, mildly blocked differentiation, dysplasia in all 3 lineages, and a slight tendency for immaturity, but no proliferation ability. Although a stem/progenitor cell with the D171N mutation is suspected to have MDS-genic potential of cell dysplasia and self-renewal capacity, it induces G1 arrest and cannot develop MDS due to lack of proliferation ability. Thus, additional gene alterations that induce proliferation activity seem to be necessary for development of MDSs. *BMI1* overexpression was suspected as a candidate collaborator because upregulated BMI1 level was observed in higher-risk MDS patients with *RUNX1* mutations, even

though the D171N mutant itself does not induce BMI1 expression. The molecular mechanism of high BMI1 expression in RUNX1-mutated patients is not due to miRNAs either. A previous study showed that forced expression of the activated *N*-RAS mutant induced overexpression of Bmi1 in mouse c-Kit$^+$ cells, especially in Runx1$^{-/-}$ cells.[39] Thus, the gene mutations that induce activation of the RAS signaling pathway, which are frequently seen in patients with *RUNX1* mutations,[40] may result at least partly in *BMI1* overexpression. Furthermore, many gene mutations have been identified in MDS patients, including PRC2 complex proteins, and some of them showed positive associations with *RUNX1* mutations.[41] Our next investigation is to clarify the effects of both expression levels and mutations of PRC2 proteins in patients with RUNX1 mutations. There is a possibility that these gene expression patterns and mutations may act to elevate the *BMI1* expression level.

BMI1 is well known to be essential for self-renewal of hematopoietic stem cells,[42-44] in part via repression of genes involved in senescence,[45] and self-renewal of hematopoietic stem cells is enhanced by BMI1 expression in both mouse and human.[35,46] Our results showed that overexpression of BMI1 itself in human CD34$^+$ cells or a mouse BMT model does not appear to have MDS-genic potential, as reported previously.[35,46] When the CD34$^+$ cells were double-transduced simultaneously with D171N and BMI1, the cells could proliferate with differentiation and dysplasia. Cotransduction of D171N and BMI1 into BM cells resulted in faster induction of MDS/AML in BMT mice. It is suggested that BMI1 overexpression may act as one of the partner abnormalities collaborating with master gene mutations for MDS genesis. BMI1 affects *INK4A/ARF* expression, which has been sufficiently elucidated, involved in the leukemic phenotype. A previous report that showed that BMI1 collaborates with BCR-ABL in leukemic transformation also supports this idea.[47] We confirmed that significant enrichments of BMI1 were detected on *Ink4a/Arf* promoter regions in both BMI1-transduced cells and BMI1/D171N-transduced cells, suggesting that BMI1 overexpression may help cells transform, at least in part, due to suppressing the expression of the *Ink4a/Arf* tumor suppressor gene. Although a physical association in vivo between BMI1 and D171N, as well as WT RUNX1,[48] was observed, it is known that the D171N mutant has lost DNA-binding ability.[12] Therefore, the mechanism by which BMI1 coexpression with the D171N mutant induces proliferative effects seems to be independent of the direct physical association between RUNX1 and BMI1. Additionally, both BMI1-knockdown human CD34$^+$ cells and *Bmi1*-deficient mouse cells showed elevated levels of reactive oxygen species accumulation,[49,50] resulting in impairment of long-term expansion and apoptosis. It may be the reason why D171N-transduced human CD34$^+$ cells that showed reduced BMI1 expression could not proliferate. It may also explain the phenomenon in 32Dcl3 cells in which BMI1 transduction seemed to rescue D171N-transduced cells from apoptosis. However, the CD34$^+$ cells transduced with D171N/BMI1 did not develop MDS/AML in NOG mice, suggesting that other factors such as *EVI1* overexpression observed in a mouse BMT model may still be required for the development of MDS/AML in NOG mice.

Germ line mutations of *RUNX1* have been shown to occur in FPD/AML.[1,2] FPD/AML is regarded as familial MDS,[3] and the molecular mechanisms by which RUNX1 mutations promote the development of hematopoietic malignancies seem to be identical in both MDS and FPD/AML patients. Because decades-long asymptomatic latency periods do occur in patients with FPD/AML, it appears that RUNX1-mutated stem cells cannot promote the development of MDSs without other cooperative factors. It is suspected that additional gene abnormalities occur later on in the RUNX1-mutated cells for the development of MDSs. Therefore, we performed stepwise transduction of the D171N mutant followed by BMI1 into CD34$^+$ cells, which could reproduce continuous slow proliferation of a low percentage of blastoid cells, reflecting the hematologic features in higher-risk MDS patients. This result indicates that genetic alterations, such as EVI1 or BMI1 overexpression, which add proliferative advantage to cells, may occur as "second hits" after the master genetic alteration (ie, RUNX1 mutation) that has MDS-genic potential.

In the present study, we revealed the functional significance of the RUNX1 D171N mutant in the pathogenesis of MDSs using human CD34$^+$ cells. Thus, amino acid replacement–type mutations in the RHD, which comprise half of the RUNX1 mutations detected in patients, are suspected to have MDS-genic potential; however, the cells with this type of mutation lack proliferation ability. This may explain BM failure status, one of the phenotypes of MDSs. When the mutated cells gain partner gene abnormality (ie, *EVI1* or *BMI1* overexpression), they can acquire proliferation ability through alteration of the collaborating gene, which may explain the various clinical features of patients with RUNX1 mutations. On the other hand, the other half of the RUNX1 mutants may have different biochemical functions that remain unclear; in particular, mutants that lack the C-terminal functional domain but have an intact RHD may have other effects.[4,22] Our future investigations include the elucidation and clarification of the molecular mechanisms by which each type of RUNX1 mutant promotes the development of MDSs.

Acknowledgments

The authors thank the pregnant women, nursing staff, and Dr Hanioka at Yamashita Clinic for providing CB and Ryoko Matsumoto-Yamaguchi for providing excellent technical support in carrying out these experiments.

This work was supported in part by Grants-in-Aid for Scientific Research from the Ministry of Education, Culture, Sports, Science and Technology of Japan; grants from Hiroshima University; a grant from the Japan Leukaemia Research Fund; and a grant from Radiation Effects Association. This work was carried out in part at the Analysis Center of Life Science, Hiroshima University.

Authorship

Contribution: Y.H. designed the research, performed experiments, and wrote the manuscript; D.I. and Y.D. performed experiments and prepared the manuscript; J.I., N.D., H. Matsui, T.Y., H. Matsushita, and G.S. collected the data; K.A., A.I., and T.K. supervised the project and discussed the results; and H.H. conceived and designed the research, collected and interpreted the data, and revised the manuscript.

Conflict-of-interest disclosure: The authors declare no competing financial interests.

Correspondence: Hironori Harada, Department of Hematology and Oncology, Research Institute for Radiation Biology and Medicine, Hiroshima University, 1-2-3 Kasumi, Minami-ku, Hiroshima 734-8553, Japan; e-mail: herf1@hiroshima-u.ac.jp.

References

1. Song WJ, Sullivan MG, Legare RD, et al. Haploinsufficiency of CBFA2 causes familial thrombocytopenia with propensity to develop acute myelogenous leukaemia. *Nat Genet.* 1999; 23(2):166-175.
2. Osato M. Point mutations in the RUNX1/AML1 gene: another actor in RUNX leukemia. *Oncogene.* 2004;23(24):4284-4296.
3. Liew E, Owen C. Familial myelodysplastic syndromes: a review of the literature. *Haematologica.* 2011;96(10):1536-1542.
4. Harada H, Harada Y, Niimi H, Kyo T, Kimura A, Inaba T. High incidence of somatic mutations in the AML1/RUNX1 gene in myelodysplastic syndrome and low blast percentage myeloid leukemia with myelodysplasia. *Blood.* 2004; 103(6):2316-2324.
5. Preudhomme C, Warot-Loze D, Roumier C, et al. High incidence of biallelic point mutations in the Runt domain of the AML1/PEBP2 alpha B gene in Mo acute myeloid leukemia and in myeloid malignancies with acquired trisomy 21. *Blood.* 2000;96(8):2862-2869.
6. Dicker F, Haferlach C, Kern W, Haferlach T, Schnittger S. Trisomy 13 is strongly associated with AML1/RUNX1 mutations and increased FLT3 expression in acute myeloid leukemia. *Blood.* 2007;110(4):1308-1316.
7. Silva FPG, Swagemakers SMA, Erpelinck-Verschueren C, et al. Gene expression profiling of minimally differentiated acute myeloid leukemia: M0 is a distinct entity subdivided by RUNX1 mutation status. *Blood.* 2009;114(14):3001-3007.
8. Tang JL, Hou HA, Chen CY, et al. AML1/RUNX1 mutations in 470 adult patients with de novo acute myeloid leukemia: prognostic implication and interaction with other gene alterations. *Blood.* 2009;114(26):5352-5361.
9. Schnittger S, Dicker F, Kern W, et al. RUNX1 mutations are frequent in de novo AML with noncomplex karyotype and confer an unfavorable prognosis. *Blood.* 2011;117(8):2348-2357.
10. Kuo MC, Liang DC, Huang CF, et al. RUNX1 mutations are frequent in chronic myelomonocytic leukemia and mutations at the C-terminal region might predict acute myeloid leukemia transformation. *Leukemia.* 2009;23(8):1426-1431.
11. Ernst T, Chase A, Zoi K, et al. Transcription factor mutations in myelodysplastic/myeloproliferative neoplasms. *Haematologica.* 2010;95(9):1473-1480.
12. Harada H, Harada Y, Tanaka H, Kimura A, Inaba T. Implications of somatic mutations in the AML1 gene in radiation-associated and therapy-related myelodysplastic syndrome/acute myeloid leukemia. *Blood.* 2003;101(2):673-680.
13. Christiansen DH, Andersen MK, Pedersen-Bjergaard J. Mutations of AML1 are common in therapy-related myelodysplasia following therapy with alkylating agents and are significantly associated with deletion or loss of chromosome arm 7q and with subsequent leukemic transformation. *Blood.* 2004;104(5):1474-1481.
14. Zharlyganova D, Harada H, Harada Y, et al. High frequency of AML1/RUNX1 point mutations in radiation-associated myelodysplastic syndrome around Semipalatinsk nuclear test site. *J Radiat Res (Tokyo).* 2008;49(5):549-555.
15. Imagawa J, Harada Y, Shimomura T, et al. Clinical and genetic features of therapy-related myeloid neoplasms after chemotherapy for acute promyelocytic leukemia. *Blood.* 2010;116(26): 6018-6022.
16. Ding Y, Harada Y, Imagawa J, Kimura A, Harada H. AML1/RUNX1 point mutation possibly promotes leukemic transformation in myeloproliferative neoplasms. *Blood.* 2009; 114(25):5201-5205.
17. Beer PA, Delhommeau F, LeCouédic JP, et al. Two routes to leukemic transformation after a JAK2 mutation-positive myeloproliferative neoplasm. *Blood.* 2010;115(14):2891-2900.
18. Zhao LJ, Wang YY, Li G, et al. Functional features of RUNX1 mutants in acute transformation of chronic myeloid leukemia and their contribution to inducing murine full-blown leukemia. *Blood.* 2012; 119(12):2873-2882.
19. Grossmann V, Kohlmann A, Zenger M, et al. A deep-sequencing study of chronic myeloid leukemia patients in blast crisis (BC-CML) detects mutations in 76.9% of cases. *Leukemia.* 2011; 25(3):557-560.
20. Tahirov TH, Inoue-Bungo T, Morii H, et al. Structural analyses of DNA recognition by the AML1/Runx-1 Runt domain and its allosteric control by CBFbeta. *Cell.* 2001;104(5):755-767.
21. Bravo J, Li Z, Speck NA, Warren AJ. The leukemia-associated AML1 (Runx1)—CBF beta complex functions as a DNA-induced molecular clamp. *Nat Struct Biol.* 2001;8(4):371-378.
22. Watanabe-Okochi N, Kitaura J, Ono R, et al. AML1 mutations induced MDS and MDS/AML in a mouse BMT model. *Blood.* 2008;111(8): 4297-4308.
23. Cattoglio C, Facchini G, Sartori D, et al. Hot spots of retroviral integration in human CD34+ hematopoietic cells. *Blood.* 2007;110(6): 1770-1778.
24. Schwieger M, Löhler J, Fischer M, Herwig U, Tenen DG, Stocking C. A dominant-negative mutant of C/EBPalpha, associated with acute myeloid leukemias, inhibits differentiation of myeloid and erythroid progenitors of man but not mouse. *Blood.* 2004;103(7):2744-2752.
25. Xu F, Li X, Wu L, et al. Overexpression of the EZH2, RING1 and BMI1 genes is common in myelodysplastic syndromes: relation to adverse epigenetic alteration and poor prognostic scoring. *Ann Hematol.* 2011;90(6):643-653.
26. Mihara K, Chowdhury M, Nakaju N, et al. Bmi-1 is useful as a novel molecular marker for predicting progression of myelodysplastic syndrome and patient prognosis. *Blood.* 2006;107(1):305-308.
27. Mulloy JC, Cammenga J, MacKenzie KL, Berguido FJ, Moore MA, Nimer SD. The AML1-ETO fusion protein promotes the expansion of human hematopoietic stem cells. *Blood.* 2002; 99(1):15-23.
28. Tonks A, Pearn L, Tonks AJ, et al. The AML1-ETO fusion gene promotes extensive self-renewal of human primary erythroid cells. *Blood.* 2003; 101(2):624-632.
29. Mulloy JC, Cammenga J, Berguido FJ, et al. Maintaining the self-renewal and differentiation potential of human CD34+ hematopoietic cells using a single genetic element. *Blood.* 2003; 102(13):4369-4376.
30. D'Costa J, Chaudhuri S, Civin CI, Friedman AD. CBFbeta-SMMHC slows proliferation of primary murine and human myeloid progenitors. *Leukemia.* 2005;19(6):921-929.
31. Wunderlich M, Krejci O, Wei J, Mulloy JC. Human CD34+ cells expressing the inv(16) fusion protein exhibit a myelomonocytic phenotype with greatly enhanced proliferative ability. *Blood.* 2006;108(5): 1690-1697.
32. Shen SW, Dolnikov A, Passioura T, et al. Mutant N-ras preferentially drives human CD34+ hematopoietic progenitor cells into myeloid differentiation and proliferation both in vitro and in the NOD/SCID mouse. *Exp Hematol.* 2004;32(9):852-860.
33. Chou FS, Wunderlich M, Griesinger A, Mulloy JC. N-Ras(G12D) induces features of stepwise transformation in preleukemic human umbilical cord blood cultures expressing the AML1-ETO fusion gene. *Blood.* 2011;117(7):2237-2240.
34. Chung KY, Morrone G, Schuringa JJ, Wong B, Dorn DC, Moore MA. Enforced expression of an Flt3 internal tandem duplication in human CD34+ cells confers properties of self-renewal and enhanced erythropoiesis. *Blood.* 2005;105(1):77-84.
35. Rizo A, Dontje B, Vellenga E, de Haan G, Schuringa JJ. Long-term maintenance of human hematopoietic stem/progenitor cells by expression of BMI1. *Blood.* 2008;111(5):2621-2630.
36. Kato N, Kitaura J, Doki N, et al. Two types of C/EBPα mutations play distinct but collaborative roles in leukemogenesis: lessons from clinical data and BMT models. *Blood.* 2011;117(1):221-233.
37. Ito M, Hiramatsu H, Kobayashi K, et al. NOD/SCID/γ(c)(null) mouse: an excellent recipient mouse model for engraftment of human cells. *Blood.* 2002;100(9):3175-3182.
38. Tsuzuki S, Hong D, Gupta R, Matsuo K, Seto M, Enver T. Isoform-specific potentiation of stem and progenitor cell engraftment by AML1/RUNX1. *PLoS Med.* 2007;4(5):e172.
39. Motoda L, Osato M, Yamashita N, et al. Runx1 protects hematopoietic stem/progenitor cells from oncogenic insult. *Stem Cells.* 2007;25(12):2976-2986.
40. Niimi H, Harada H, Harada Y, et al. Hyperactivation of the RAS signaling pathway in myelodysplastic syndrome with AML1/RUNX1 point mutations. *Leukemia.* 2006;20(4):635-644.
41. Bejar R, Stevenson K, Abdel-Wahab O, et al. Clinical effect of point mutations in myelodysplastic syndromes. *N Engl J Med.* 2011; 364(26):2496-2506.
42. van der Lugt NM, Domen J, Linders K, et al. Posterior transformation, neurological abnormalities, and severe hematopoietic defects in mice with a targeted deletion of the bmi-1 proto-oncogene. *Genes Dev.* 1994;8(7):757-769.
43. Park IK, Qian D, Kiel M, et al. Bmi-1 is required for maintenance of adult self-renewing haematopoietic stem cells. *Nature.* 2003; 423(6937):302-305.
44. Lessard J, Sauvageau G. Bmi-1 determines the proliferative capacity of normal and leukaemic stem cells. *Nature.* 2003;423(6937):255-260.
45. Jacobs JJ, Kieboom K, Marino S, DePinho RA, van Lohuizen M. The oncogene and Polycomb-group gene bmi-1 regulates cell proliferation and senescence through the ink4a locus. *Nature.* 1999;397(6715):164-168.
46. Iwama A, Oguro H, Negishi M, et al. Enhanced self-renewal of hematopoietic stem cells mediated by the polycomb gene product Bmi-1. *Immunity.* 2004;21(6):843-851.
47. Rizo A, Horton SJ, Olthof S, et al. BMI1 collaborates with BCR-ABL in leukemic transformation of human CD34+ cells. *Blood.* 2010;116(22):4621-4630.
48. Yu M, Mazor T, Huang H, et al. Direct recruitment of polycomb repressive complex 1 to chromatin by core binding transcription factors. *Mol Cell.* 2012; 45(3):330-343.
49. Rizo A, Olthof S, Han L, Vellenga E, de Haan G, Schuringa JJ. Repression of BMI1 in normal and leukemic human CD34(+) cells impairs self-renewal and induces apoptosis. *Blood.* 2009; 114(8):1498-1505.
50. Liu J, Cao L, Chen J, et al. Bmi1 regulates mitochondrial function and the DNA damage response pathway. *Nature.* 2009;459(7245): 387-392.